

University of Groningen

## Atomic stacking and van-der-Waals bonding in GeTe-Sb<sub>2</sub>Te<sub>3</sub> superlattices

Momand, Jamo; Lange, Felix R. L.; Wang, Ruining; Boschker, Jos E.; Verheijen, Marcel A.; Calarco, Raffaella; Wuttig, Matthias; Kooi, Bart J.

*Published in:*  
Journal of materials research

*DOI:*  
[10.1557/jmr.2016.334](https://doi.org/10.1557/jmr.2016.334)

**IMPORTANT NOTE:** You are advised to consult the publisher's version (publisher's PDF) if you wish to cite from it. Please check the document version below.

*Document Version*  
Publisher's PDF, also known as Version of record

*Publication date:*  
2016

[Link to publication in University of Groningen/UMCG research database](#)

*Citation for published version (APA):*

Momand, J., Lange, F. R. L., Wang, R., Boschker, J. E., Verheijen, M. A., Calarco, R., Wuttig, M., & Kooi, B. J. (2016). Atomic stacking and van-der-Waals bonding in GeTe-Sb<sub>2</sub>Te<sub>3</sub> superlattices. *Journal of materials research*, 31(20), 3115-3124. <https://doi.org/10.1557/jmr.2016.334>

### Copyright

Other than for strictly personal use, it is not permitted to download or to forward/distribute the text or part of it without the consent of the author(s) and/or copyright holder(s), unless the work is under an open content license (like Creative Commons).

The publication may also be distributed here under the terms of Article 25fa of the Dutch Copyright Act, indicated by the "Taverne" license. More information can be found on the University of Groningen website: <https://www.rug.nl/library/open-access/self-archiving-pure/taverne-amendment>.

### Take-down policy

If you believe that this document breaches copyright please contact us providing details, and we will remove access to the work immediately and investigate your claim.

*Downloaded from the University of Groningen/UMCG research database (Pure): <http://www.rug.nl/research/portal>. For technical reasons the number of authors shown on this cover page is limited to 10 maximum.*

# Atomic stacking and van-der-Waals bonding in GeTe–Sb<sub>2</sub>Te<sub>3</sub> superlattices

Jamo Momand<sup>a)</sup>

Zernike Institute for Advanced Materials, University of Groningen, 9747 AG Groningen, The Netherlands

Felix R.L. Lange

I. Physikalisches Institut (IA), RWTH Aachen University, 52056 Aachen, Germany; and JARA-Institut Green IT, Forschungszentrum Jülich GmbH and RWTH Aachen University, 52056 Aachen, Germany

Ruining Wang and Jos E. Boschker

Department of Epitaxy, Paul-Drude-Institut für Festkörperelektronik, 10117 Berlin, Germany

Marcel A. Verheijen

Eindhoven University of Technology, Department of Applied Physics, NL-5600 MB Eindhoven, The Netherlands

Raffaella Calarco

Department of Epitaxy, Paul-Drude-Institut für Festkörperelektronik, 10117 Berlin, Germany

Matthias Wuttig

I. Physikalisches Institut (IA), RWTH Aachen University, 52056 Aachen, Germany; and JARA-Institut Green IT, JARA-FIT, Forschungszentrum Jülich GmbH and RWTH Aachen University, 52056 Aachen, Germany

Bart J. Kooi<sup>b)</sup>

Zernike Institute for Advanced Materials, University of Groningen, 9747 AG Groningen, The Netherlands

(Received 30 May 2016; accepted 26 August 2016)

GeTe–Sb<sub>2</sub>Te<sub>3</sub> superlattices have attracted major interest in the field of phase-change memories due to their improved properties compared with their mixed counterparts. However, their crystal structure and resistance-switching mechanism are currently not clearly understood. In this work epitaxial GeTe–Sb<sub>2</sub>Te<sub>3</sub> superlattices have been grown with different techniques and were thoroughly investigated to unravel the structure of their crystalline state with particular focus on atomic stacking and van-der-Waals bonding. It is found that, due to the bonding anisotropy of GeTe and Sb<sub>2</sub>Te<sub>3</sub>, the materials intermix to form van-der-Waals heterostructures of Sb<sub>2</sub>Te<sub>3</sub> and stable GeSbTe. Moreover, it is found through annealing experiments that intermixing is stronger for higher temperatures. The resulting ground state structure contradicts the dominant ab-initio results in the literature, requiring revisions of the proposed switching mechanisms. Overall, these findings shed light on the bonding nature of GeTe–Sb<sub>2</sub>Te<sub>3</sub> superlattices and open a way to the understanding of their functionality.

## I. INTRODUCTION

The materials on the ternary phase-diagram of GeSbTe show an extraordinary combination of physical properties: many of these alloys can be switched rapidly and reversibly between their amorphous and crystalline phases, having large differences in optical reflectivity or electrical resistivity, but at the same time remain remarkably stable at room temperature.<sup>1–4</sup> It is for these reasons that phase-change materials (PCMs) of GeSbTe alloys (bulk GeSbTe), most notably Ge<sub>2</sub>Sb<sub>2</sub>Te<sub>5</sub>, have been applied in optical recording media like rewritable disks, and are currently intensely investigated for next-generation nonvolatile

electronic memories<sup>5,6</sup> and opto-electronic applications.<sup>7–9</sup> Moreover, PCMs have recently attracted scientific interest due to the occurrence of a controlled insulator–metal transition upon annealing the crystalline phase, which is shown to be of an Anderson (and not Mott) type.<sup>10</sup> This makes GeSbTe based PCMs also an interesting platform for fundamental studies on transport and charge localization.

For PCM electronic memories one of the major drawbacks is the large programming current ( $I_{\text{prog}}$ ) which is needed for reset switching (i.e., amorphization) of the material. The reason is that  $I_{\text{prog}}$  is coupled to the memory's crystalline resistance ( $R_{\text{set}}$ ) in an inversely proportional way, typically  $I_{\text{prog}} \sim R_{\text{set}}^{-1}$ , which particularly becomes important as the devices are being scaled to lower dimensions.<sup>11,12</sup> A breakthrough in the field occurred when Chong et al. and later Simpson et al. showed that thin films consisting of GeTe–Sb<sub>2</sub>Te<sub>3</sub> multilayers and superlattices, produced in rather different

Contributing Editor: Gary L. Messing

Address all correspondence to these authors.

<sup>a)</sup>e-mail: j.momand@rug.nl

<sup>b)</sup>e-mail: b.j.kooi@rug.nl

This paper has been selected as an Invited Feature Paper.

DOI: 10.1557/jmr.2016.334

ways, have significantly reduced  $I_{\text{prog}}$  compared to bulk GeSbTe, as well as new and better switching properties.<sup>13,14</sup> Chong et al. initially proposed that the reduced programming current originates from the lower thermal conductivity of the super-structure. However, this suggestion was disputed for the epitaxial films with much thinner GeTe sublayers in the work by Simpson et al., referred to as interfacial phase-change memory (iPCM), who showed using pump-probe thermorefectivity that this conductivity was actually higher for superlattices than for bulk GeSbTe. This led the authors to seek an explanation in terms of a crystal–crystal transition in iPCM,<sup>15,16</sup> skipping the costly amorphization step (via the molten state), and thereby reducing  $I_{\text{prog}}$ .

Despite these advances, the structural models and resistance-switching mechanism of iPCM are not clearly understood and different theories are debated in the literature. In this work, as well as in previous publications,<sup>17–19</sup> we critically analyze the atomic structure of epitaxial GeTe–Sb<sub>2</sub>Te<sub>3</sub> superlattice PCMs with special attention to (i) ordering and mixing of Ge and Sb and (ii) the formation of so-called vacancy layers and van-der-Waals (vdW) bonds. Using both molecular beam epitaxy (MBE) and sputtering physical vapor deposition (PVD) various superlattice films were grown and characterized with high-resolution (HR) transmission electron microscopy (TEM), high-angle annular dark field scanning TEM (HAADF-STEM), TEM energy dispersive x-ray spectroscopy (EDX), and x-ray diffraction (XRD). Contrary to the proposed models in the field of iPCM, it is found that the separate binary compounds intermix and actually form superlattices of Sb<sub>2</sub>Te<sub>3</sub> and GeSbTe vdW layers, as would be expected based on the structural models by Kooi et al.<sup>20</sup> and Matsunaga et al.<sup>21–23</sup>

## II. CRYSTAL STRUCTURES OF GeTe, Sb<sub>2</sub>Te<sub>3</sub> AND GeSbTe

To better understand the properties and the proposed resistance-switching mechanisms of GeTe–Sb<sub>2</sub>Te<sub>3</sub> superlattices, as well as PCMs on the GeTe–Sb<sub>2</sub>Te<sub>3</sub> tie-line, it is necessary to study the crystalline structure and bonding of the ternary as well as the separate binary compounds. Figures 1(a)–1(c) show the structural models of GeTe, Sb<sub>2</sub>Te<sub>3</sub> and the stable phase of Ge<sub>2</sub>Sb<sub>2</sub>Te<sub>5</sub> (s-Ge<sub>2</sub>Sb<sub>2</sub>Te<sub>5</sub>) according to Goldak et al.,<sup>24</sup> Anderson et al.,<sup>25</sup> and Kooi et al.,<sup>20</sup> respectively. As can be seen in the figures, all structures are based on consecutive abc-stacking of close-packed atomic planes. Within a simplified picture, GeTe is a three-dimensionally (3D) bonded solid which has approximately a rocksalt structure that is rhombohedrally and ferroelectrically distorted along one of the four  $\langle 111 \rangle$  directions ( $c > a\sqrt{6}$  and  $z = 0.237$ , where  $c = a\sqrt{6}$  and  $z = 0.250$  for the rocksalt structure). Sb<sub>2</sub>Te<sub>3</sub> on the other hand has an additional feature of directly adjacent Te–Te

planes stacked upon each other, which breaks the rocksalt symmetry by breaking the super-ABC stacking of the Te planes. This happens since Sb has one extra valence electron, and because of this the bonds on the outer Te planes are passivated and form two-dimensional (2D) vdW bonds. This type of vdW bond, which also occurs in e.g., graphene-based materials and transition-metal di-chalcogenides,<sup>26</sup> is referred to as vdW gap. Note that, although Sb<sub>2</sub>Te<sub>3</sub> has certainly a more 2D than 3D anisotropy, the Te–Te bond does not necessarily have to be of pure vdW type (e.g., the Te–Te interatomic distance is a bit smaller than what would be expected based on the vdW radius<sup>21–23</sup>). Considering the above, the model for s-Ge<sub>2</sub>Sb<sub>2</sub>Te<sub>5</sub> by Kooi et al. takes into account this 3D and 2D character of GeTe and Sb<sub>2</sub>Te<sub>3</sub>, respectively, and fitted best to experimental electron diffraction results at that time.<sup>20</sup>

When GeSbTe crystallizes from the amorphous phase, it initially forms a metastable rocksalt structure (m-GeSbTe), where one sublattice is fully occupied with Te and the other sublattice is randomly occupied by Ge, Sb and a large amount of stoichiometric vacancies ( $\sim 20\%$  for Ge<sub>2</sub>Sb<sub>2</sub>Te<sub>5</sub>),<sup>27,28</sup> see Fig. 1(d). To make the transition from m-GeSbTe to s-GeSbTe it has been suggested that the mechanism involves atomic diffusion of Ge and Sb in such a way that the vacancies order in layers and consequently collapse into vdW gaps.<sup>21,29</sup> Note particularly the difference in stacking between vacancy layers and vdW gaps in Fig. 1(d). An appreciable amount of disorder on the Ge/Sb planes nevertheless remains after this transition: even though the structure of s-GeSbTe best fits the model of Kooi et al. with Sb–Te directly at the vdW gaps, it was found by Matsunaga et al. using Rietveld refinement on XRD spectra that the Ge-rich planes are mixed with Sb and Sb-rich planes with Ge.<sup>21–23</sup> In later ab-initio studies relating to the ordering of vacancies it was indeed found that the pure atomic-plane model by Kooi et al. gives the lowest formation energy (at zero Kelvin), but that mixing only slightly increases this energy.<sup>30</sup> Therefore, due to this low energy increase and the free energy decrease due to configurational entropy, which becomes increasingly relevant at higher temperatures, the stable phase of bulk GeSbTe is always found with some degree of mixing on the Ge/Sb atomic planes (at practical temperatures particularly dictated by production), but with the Sb-rich planes nearest to the vdW gaps.

For GeTe–Sb<sub>2</sub>Te<sub>3</sub> superlattices the separate binary compounds are deposited alternately, which hypothetically could produce pure atomic planes. In addition, since Sb<sub>2</sub>Te<sub>3</sub> grows in entire 1 nm quintuple layer (QL) terraces,<sup>31</sup> preferring to form layers with passive vdW surfaces, it could be possible to isolate ultra-thin GeTe layers between the vdW surfaces of Sb<sub>2</sub>Te<sub>3</sub>. In combination with the research on superlattices and understanding



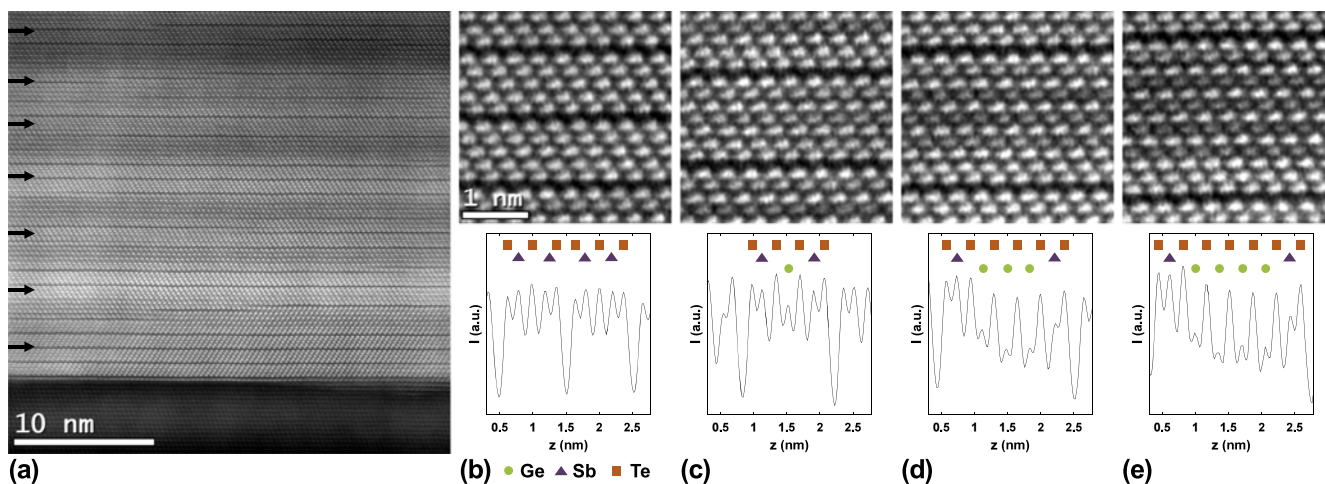


FIG. 2. HAADF-STEM results of MBE grown [GeTe(1 nm)–Sb<sub>2</sub>Te<sub>3</sub>(3 nm)]<sub>15</sub> superlattice on Si(111)-Sb. Above the intensity scans it is indicated whether the atomic plane is Ge-, Sb- or Te-rich with circles, triangles and squares, respectively. (a) Overview image of the superlattice. (b) 5-layers corresponding to Sb<sub>2</sub>Te<sub>3</sub>. (c) 7-layer. (d) 11-layer. (e) 13-layer.

to form the Sb–Te termination that is establishing the vdW bond.

In addition, stacking faults and layering disorder occur in the film, which is best seen by the 2- or 4-layered stacking faults in between the odd-layered vdW systems in the film in Fig. 2(a). This is indicative of growth roughness, which is an inherent experimental feature of the growth of these materials. These stacking faults are also another indication that the film has a strong tendency to reconfigure itself. All these findings of the formed vdW layers and defects are fully consistent with the models for s-GeSbTe as proposed by Kooi et al. and Matsunaga et al. Hence, the ground state crystal structure of GeTe–Sb<sub>2</sub>Te<sub>3</sub> superlattices is actually better described as vdW heterostructures of Sb<sub>2</sub>Te<sub>3</sub> and s-GeSbTe.

## B. PVD grown superlattices

PVD is another technique for film-growth with the advantage that it is adopted much more easily in an industrial process than MBE. Beside this, most of the previous results in the literature have been achieved using PVD grown GeTe–Sb<sub>2</sub>Te<sub>3</sub> films.<sup>13,14,33,34</sup> Figure 3 shows (coherent) HRTEM micrographs of a [GeTe(4 nm)–Sb<sub>2</sub>Te<sub>3</sub>(3 nm)]<sub>15</sub> superlattice, produced at 210 °C with PVD. The film is grown on H-passivated Si(111) which is the surface formed after an HF treatment of the substrate. Also in this case a strong substrate-film alignment occurs, as will be shown in more detail below. HRTEM has a different contrast mechanism than HAADF-STEM because the images are formed through coherent interference of electrons (phase contrast) and this makes interpretation typically more difficult and not directly Z-sensitive. However, due to the dimensionality difference of GeTe and Sb<sub>2</sub>Te<sub>3</sub> it is still possible to

distinguish the QLs, and sometimes 7-layers, within the film as can be observed in Fig. 3(a).

Figure 3(b) shows a close-up micrograph of the sublayers that are formed, which seem to disagree with the intended GeTe(4 nm)–Sb<sub>2</sub>Te<sub>3</sub>(3 nm) thicknesses. The GeTe sublayer appears to be 5 nm, while only 2 nm (2 QLs) of Sb<sub>2</sub>Te<sub>3</sub> are observed. The bilayer thickness is also verified with EDX, which resulted on average in 29.2 ± 0.5 at.% Ge, 15.3 ± 0.7 at.% Sb and 55.5 ± 0.9 at.% Te. This is equivalent to 61.6 ± 0.9 at.% Ge<sub>47</sub>Te<sub>53</sub> and 38.4 ± 0.7 at.% Sb<sub>2</sub>Te<sub>3</sub>, where GeTe is a bit off-stoichiometric due to the inherent presence of ~10% vacancies on the Ge lattice.<sup>37</sup> Using these compositional results and the fact that the ~110 nm film is highly textured along the c-axis, which allows using the literature distances for GeTe (0.356 nm/bilayer), Sb<sub>2</sub>Te<sub>3</sub> (0.1015 nm/QL) and s-GeSbTe, it is calculated that the film on average contains 4.3 nm GeTe and 2.7 nm Sb<sub>2</sub>Te<sub>3</sub>. So since 2 nm of Sb<sub>2</sub>Te<sub>3</sub> have formed 5-layered vdW systems (QLs) the remaining amount of Sb is used in the termination of the GeTe sublayers, which is needed to form the vdW bond, as illustrated by the model in Fig. 3(b) on the right. Therefore, also these results of thicker GeTe–Sb<sub>2</sub>Te<sub>3</sub> superlattices produced by sputtering clearly support the formation of s-GeSbTe with mixed Sb-rich planes next to the vdW gap.

## C. Thermal stability of GeTe–Sb<sub>2</sub>Te<sub>3</sub> superlattices

The study of the thermal stability of the superlattices is important because (i) it is argued that there is a thermodynamic tendency to form isolated GeTe blocks within Sb<sub>2</sub>Te<sub>3</sub> at elevated temperatures<sup>33,35,38</sup> and (ii) for industrial applications the material has to be able to withstand a certain amount of thermal processing. Beside this, growth at elevated temperatures above ~200 °C is

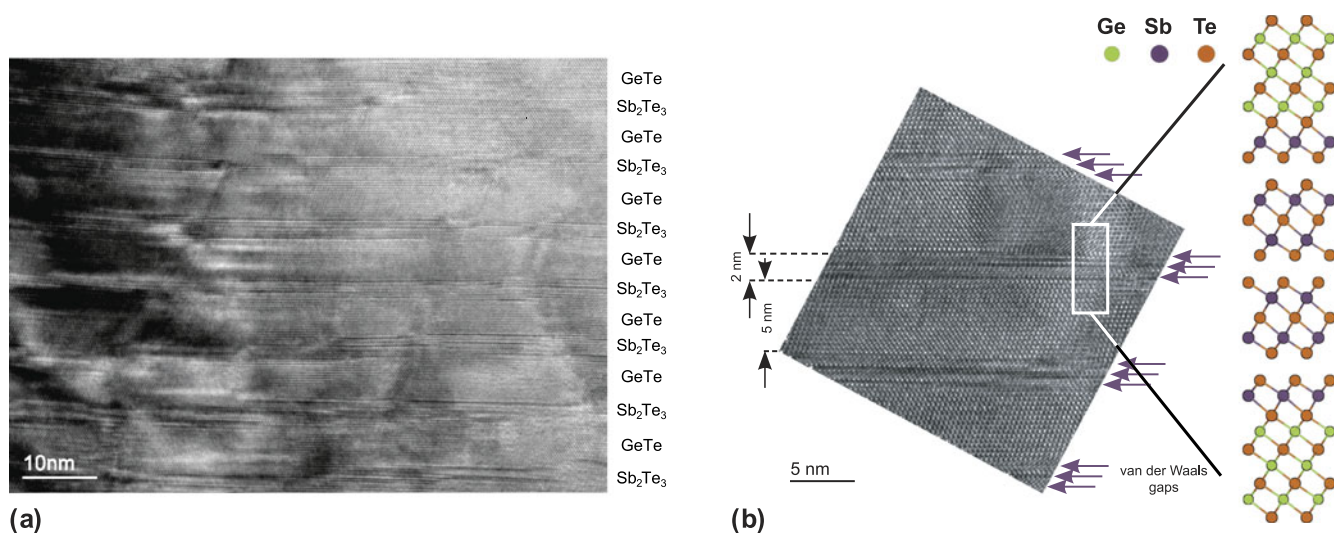


FIG. 3. HRTEM results of PVD grown [GeTe(4 nm)–Sb<sub>2</sub>Te<sub>3</sub>(3 nm)]<sub>15</sub> superlattice on Si(111)-H. (a) Overview image of the superlattice. (b) High-resolution image of the superlattice. The model for the structure that is formed is indicated on the right of the image.

required for textured growth to occur.<sup>14</sup> As it was already shown above, that for growth around  $\sim 230$  °C the separate binary compounds intermix by terminating the GeTe blocks with Sb–Te vdW surfaces, it is interesting to know what the further development is at higher temperatures. To examine this a set of [GeTe(1 nm)–Sb<sub>2</sub>Te<sub>3</sub>(3 nm)]<sub>15</sub> superlattices were prepared on Si(111)-H with PVD at 210 °C and capped with ZnS:SiO<sub>2</sub> (80:20) to prevent preferential evaporation of GeTe during annealing. Additionally a GeSb<sub>2</sub>Te<sub>4</sub> film was grown from a stoichiometric target at 320 °C on mica substrates for comparison of the overall structure. Figure 4(a) shows the  $\theta$ – $2\theta$  XRD results of the as-deposited and 250, 300, 350 and 400 °C annealed films.

The as-deposited film clearly shows superlattice peaks at  $Q_z = 1.816 \text{ \AA}^{-1}$  and  $Q_z = 3.635 \text{ \AA}^{-1}$ , as well as the 250 °C annealed film which hardly changed the as-deposited structure. However, new and distinct peaks of equally spaced  $Q_z$  appear after annealing temperature of 350 °C, which further develop at 400 °C. Comparing the positions as well as the intensities of all peaks with the GeSb<sub>2</sub>Te<sub>4</sub> film on mica, it becomes apparent that the superlattice has reconfigured into s-GeSb<sub>2</sub>Te<sub>4</sub>, as is schematically illustrated in Fig. 4(b). This finding for the present PVD grown films is fully consistent and in line with the previously obtained results for the MBE grown ones.<sup>17</sup> It implies that the intermixing of GeTe and Sb<sub>2</sub>Te<sub>3</sub> to form s-GeSbTe is a thermodynamic tendency and that this becomes more pronounced at higher annealing or deposition temperatures such that the superlattice feature is lost after 30 min. annealing at 350 or 400 °C. This outlines a delicate thermal balance which has to be achieved during growth: the temperature has to be high enough to favor texture of the superlattice

material, but at the same time it has to be low enough to maintain sharp interfaces. Moreover, this shows that the superlattice materials have a limited thermal budget which they can handle, which has to be taken into account for potential industrial implementation. Overall, these findings thus disagree with the previously mentioned ab-initio results<sup>33,35,38</sup> and suggest that configurational entropy due to mixing, particularly of the Ge/Sb atomic planes, has to be taken into account for the modeling.

#### D. Surface preparation

An important prerequisite for the growth of GeTe–Sb<sub>2</sub>Te<sub>3</sub> superlattices is the ability to achieve a film with large domains and a sharp texture due to a single [0001] out-of-plane orientation of the trigonal structure, which typically occurs at deposition temperatures above  $\sim 200$  °C.<sup>14</sup> Also here, several theories exist on what is the best way to achieve this based on the chemistry of the relevant materials.<sup>36,39</sup> Since Sb<sub>2</sub>Te<sub>3</sub> is a 2D bonded component of the film, preferring to organize itself in entire QLs, it becomes natural to exploit this property using vdW epitaxy.<sup>40</sup> This approach has the additional advantage that the lattice-matching condition is much more relaxed than for 3D epitaxy, as the chemical bonding on the surface is much weaker. This is the reason why in the above experiments either Si(111)-Sb and Si(111)-H surfaces have been applied. Using these passive surfaces and the Sb<sub>2</sub>Te<sub>3</sub> starting layer, it is possible to grow highly textured and substrate-oriented films.<sup>36</sup> Figure 5(a) shows an experimental XRD pole figure of the Si(111)-H PVD grown superlattice from Fig. 3 along the {01–12} peak family (conducted at

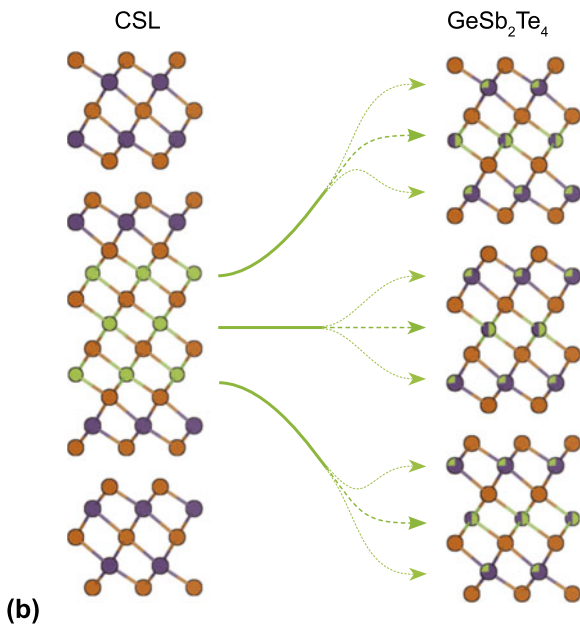
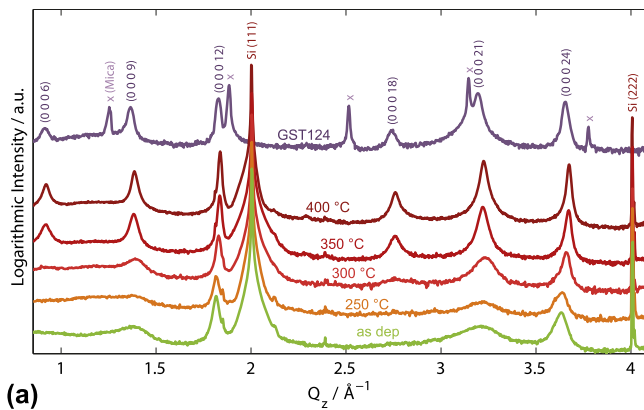


FIG. 4. XRD results of thermal annealing experiments with PVD grown [GeTe(1 nm)–Sb<sub>2</sub>Te<sub>3</sub>(3 nm)]<sub>15</sub>. (a)  $\theta$ – $2\theta$  scans of the superlattice at different temperatures in comparison with GeSb<sub>2</sub>Te<sub>4</sub> which is directly deposited on Mica (top scan). The results clearly indicate that the superlattice structure thermally reconfigures into bulk GeSb<sub>2</sub>Te<sub>4</sub> after 350 °C. (b) Illustration of the structural models for the [GeTe(1 nm)–Sb<sub>2</sub>Te<sub>3</sub>(3 nm)] superlattice (CSL) (left)<sup>17,18</sup> which reconfigures into the stable phase of bulk GeSb<sub>2</sub>Te<sub>4</sub> (right).<sup>21</sup>

$2\theta = 29.80^\circ$  or  $|Q| = 2.098 \text{ \AA}^{-1}$ ). From the figure it is clear that the superlattice not only has an excellent out-of-plane alignment, but it is also in-plane aligned with the Si substrate. Since the crystal structure of the superlattice is trigonal, the hexagonal pattern is the result of crystal twinning ( $60^\circ$  or  $180^\circ$  rotation around the  $[0001]$  i.e., perpendicular to the interface). This epitaxy is schematically illustrated (by a simplified geometric model, excluding potential matching strains which will be small for this vdW-like epitaxy) in Fig. 5(b), where the last (111) plane of Si and the first Te plane of an Sb<sub>2</sub>Te<sub>3</sub> quintuple relative to the interface are overlaid on top of each other.

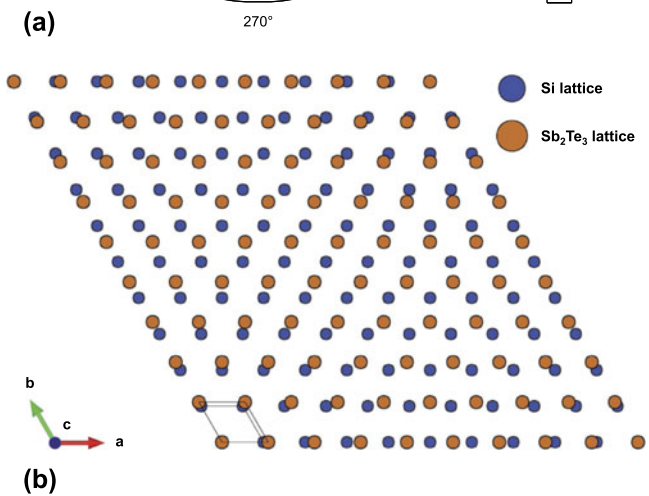
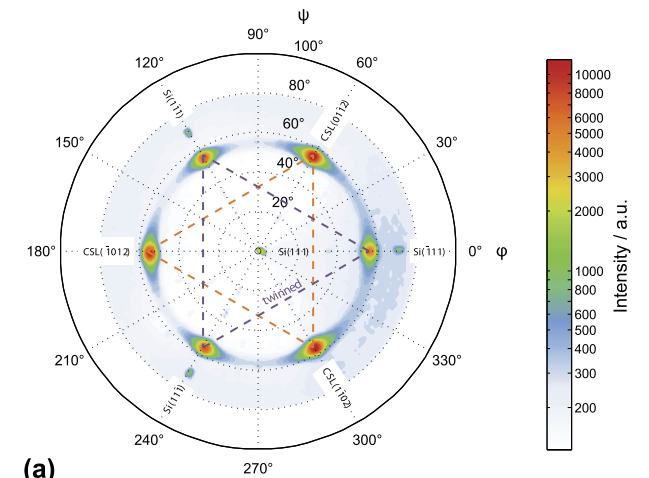


FIG. 5. Epitaxial matching between Si(111) and GeTe–Sb<sub>2</sub>Te<sub>3</sub> superlattices. (a) XRD pole figure of the Si(111)-H PVD grown superlattice showing the  $\{01-12\}$  peak family (conducted at  $2\theta = 29.80^\circ$  or  $|Q| = 2.098 \text{ \AA}^{-1}$ ). The result shows that the superlattice not only has a good out-of-plane alignment, but it is also in-plane aligned with the Si substrate. Since the crystal structure of the superlattice is trigonal, the hexagonal pattern is the result of crystal twinning. (b) Schematic overlay of the nearest close-packed planes of the Si and Sb<sub>2</sub>Te<sub>3</sub> lattices, illustrating the dominant epitaxial relationship according to (a).

Thus, a significant feature for lateral Sb<sub>2</sub>Te<sub>3</sub> growth is that the starting surface is passive, but also smooth, which does not imply that the surface has to be crystalline. This is shown for PVD grown Sb<sub>2</sub>Te<sub>3</sub> layers on the native oxide of the Si substrate. Figure 6(a) shows a part of the film where the native oxide is relatively flat and therefore the quintuple structures of Sb<sub>2</sub>Te<sub>3</sub> can properly organize. This happens during growth initiation to minimize dangling bond surfaces and maximize the passive vdW surface. However, if the surface is rough, tilted domains can form and are observed; see an example shown in Fig. 6(b). The tilt occurs because the initial QLs are formed with a tilt on the rough surface and this is a further seed for subsequent growth. Therefore, the surface roughness is of crucial importance for the growth

of superlattices, consistent with the findings by Saito et al.,<sup>39</sup> who suggest a way to achieve it with ion-polishing (to produce an amorphous Si surface). Still, in the work of Saito et al. it is claimed that high quality lateral growth also requires materials at the surface that have preference to bond to Te and not Sb. In this respect silicon oxide would not be a suitable surface. However, the present work shows, as has also been pointed out by Ross et al.,<sup>41</sup> that it is nevertheless possible to achieve lateral Sb<sub>2</sub>Te<sub>3</sub> growth on SiO<sub>2</sub> directly, indicating that it is rather the surface chemistry than bulk chemistry which is dominant for growth.

#### IV. DISCUSSION

In the above results it is shown that for both MBE and PVD grown superlattices the separate binary GeTe and Sb<sub>2</sub>Te<sub>3</sub> layers intermix. This implies that part of the Sb<sub>2</sub>Te<sub>3</sub> sublayer is used to terminate the GeTe blocks to form passive vdW surfaces. When approaching the ultrathin GeTe limit, this type of surface termination thus naturally forms s-GeSbTe blocks, of which an example is shown in Fig. 1(c) for s-Ge<sub>2</sub>Sb<sub>2</sub>Te<sub>5</sub>. Therefore, these findings implicate that the ground state of GeTe–Sb<sub>2</sub>Te<sub>3</sub> superlattices is best described as a superstructure, i.e., a vdW heterostructure, of Sb<sub>2</sub>Te<sub>3</sub> and s-GeSbTe. In addition, it has been shown through annealing experiments that GeTe–Sb<sub>2</sub>Te<sub>3</sub> intermixing becomes more favorable upon higher temperature. This can even reconfigure the superlattice films entirely into bulk s-GeSbTe if the deposition or annealing temperature is sufficiently high (e.g., 400 °C). Thus, this is an important constraint which is put on growth and processing of the GeTe–Sb<sub>2</sub>Te<sub>3</sub> superlattices, both in terms of film production as well as industrial implementation (which requires heating for several other processing steps).

The proposed ground state for GeTe–Sb<sub>2</sub>Te<sub>3</sub> superlattices, a vdW heterostructure of s-GeSbTe and Sb<sub>2</sub>Te<sub>3</sub>, is contradictory to the modeled structures proposed in the literature,<sup>33,34,38</sup> where it is suggested that GeTe can be isolated within the vdW surfaces of Sb<sub>2</sub>Te<sub>3</sub> layers. The implication of this is that the proposed switching mechanisms, as illustrated in Fig. 1(e), cannot hold or cannot present the complete picture, because they require the previously mentioned condition of GeTe directly adjacent to neighboring Te planes which in principle are the vdW gaps. A possible reason for these discrepancies in the modeling could be the assumption that all structural models consist of pure atomic planes. The work on bulk GeSbTe by Matsunaga et al.,<sup>21–23</sup> already showed that this assumption is incorrect. Therefore, these ab-initio simulations omit the important contribution of configurational entropy to the free energy. This contribution becomes more important at higher temperatures, which are within the growth/annealing regime under consideration.

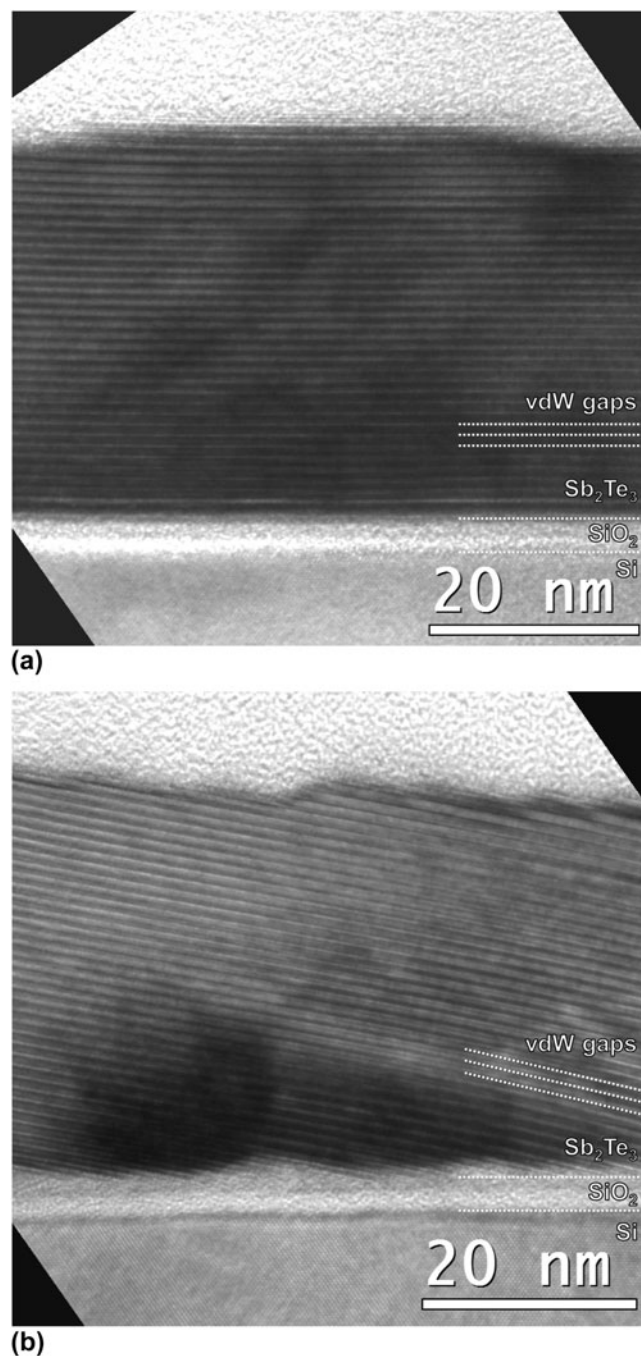


FIG. 6. Sb<sub>2</sub>Te<sub>3</sub> films grown with PVD on the native oxide of Si(100). (a) Part of the film which shows good out-of-plane alignment due to the smooth SiO<sub>2</sub> starting surface. This can be seen since the vdW gaps of Sb<sub>2</sub>Te<sub>3</sub> are aligned parallel to the interface. (b) Part of the film which shows a tilted domain, recognized by the tilted vdW gaps of Sb<sub>2</sub>Te<sub>3</sub>, which has formed on a rough part of the substrate.

In addition, the switching models here are always considering only 2 GeTe bilayers.<sup>33,34,38</sup> This is a tough experimental challenge as in practice one always has to take into account roughness, as shown in the current results, and GeTe re-evaporation which is present at



higher temperatures.<sup>42,43</sup> Since it is shown that the superlattices operate at higher sublayer thicknesses of 4 GeTe bilayers,<sup>14</sup> it remains unclear how the switching mechanisms generalize to these conditions.

Therefore, it is debatable whether the proposed switching mechanisms in the literature are correct and can explain the properties of GeTe–Sb<sub>2</sub>Te<sub>3</sub> superlattices. A possible alternative, as also pointed out in our previous work,<sup>17</sup> relates to the conventional amorphous-crystalline phase transition of ultrathin GeSbTe layers clamped in the Sb<sub>2</sub>Te<sub>3</sub> matrix. However, one still has to explain the reduced energy consumption which is found in this material. One aspect that is reviving is the improved thermal efficiency (due to the many interfaces) of the superlattice compared to bulk GeSbTe. Such a reduction in thermal conductivity as compared to the constituent materials and also the alloyed compound appears to be a fingerprint of superlattice structures and is also reported in chemically similar systems such as Sb<sub>2</sub>Te<sub>3</sub>–Bi<sub>2</sub>Te<sub>3</sub><sup>44</sup> or PbTe–PbTe<sub>0.75</sub>Se<sub>0.25</sub>.<sup>45</sup> Moreover, as also pointed out previously, a possible solution could lie in the strain which is built up in the sublayers, as can be deduced from the *a*-lattice constants of GeTe, *s*-Ge<sub>3</sub>Sb<sub>2</sub>Te<sub>6</sub>, *s*-Ge<sub>2</sub>Sb<sub>2</sub>Te<sub>5</sub>, *s*-GeSb<sub>2</sub>Te<sub>4</sub>, Sb<sub>2</sub>Te<sub>3</sub> which are *a* = 0.417, 0.421, 0.422, 0.423, 0.426 nm, respectively.<sup>21–25</sup> Such distortions may add to the total energy of the crystal and thereby lower the amorphization energy,<sup>46</sup> while the faster crystallization dynamics could be explained by templated growth.<sup>47</sup> This type of strain engineering is being suggested by Simpson et al., who propose to use an Sb<sub>2</sub>Te spacer instead of Sb<sub>2</sub>Te<sub>3</sub>.<sup>48</sup> Because of the larger strain due to the larger *a*-constant of Sb<sub>2</sub>Te the memory cells showed even lower energy consumption.

## V. CONCLUSIONS

In this work it is shown that the ground state of GeTe–Sb<sub>2</sub>Te<sub>3</sub> superlattices is actually better described as a vdW heterostructure of Sb<sub>2</sub>Te<sub>3</sub> and stable GeSbTe, irrespective of the growth method (MBE or sputtering). The formation of the stable GeSbTe blocks like the one shown in Fig. 1(c), occurs due to the tendency of GeTe to intermix with Sb<sub>2</sub>Te<sub>3</sub> and thereby form passivated vdW surfaces. This type of surface appears to be energetically more favorable over surfaces containing dangling bonds, which is why it seems not possible to obtain isolated blocks of GeTe between Sb<sub>2</sub>Te<sub>3</sub>. In addition, it has been shown that intermixing is a thermodynamic tendency which becomes stronger for higher temperatures. This highlights the delicate thermal balance which has to be achieved during growth: the temperature should be sufficiently high to have high-textured crystalline growth but not so high to prevent bulk intermixing and alloying.

The experimental results in this work are thus in striking contradiction with some of the ab-initio results

by Tominaga et al. and Ohyanagi et al., which argue that intermixing of GeTe and Sb<sub>2</sub>Te<sub>3</sub> is weaker for higher deposition temperatures. In addition, this type of modeling only takes into account structures with pure atomic planes, omitting the important contributions due to configurational entropy to the free energy of GeSbTe at higher temperatures. Because of this it seems unlikely that the proposed structural models of GeTe–Sb<sub>2</sub>Te<sub>3</sub> superlattices form experimentally and thus that the proposed switching mechanisms are correct. Therefore it becomes necessary to revise the switching model of the GeSbTe superlattices taking into account Sb-rich (instead of Ge) planes near the vdW gaps.

The study of GeTe–Sb<sub>2</sub>Te<sub>3</sub> interfaces in addition provides a versatile platform for the study of the physical phenomena in GeSbTe alloys, such as the formation of vacancy layers, vdW bonds and the related metal-insulator transition which occurs due to ordering. It shows the interplay of different bonding dimensionalities which is tunable within GeSbTe. Overall, the present results have important implications for the understanding of the bonding in GeTe–Sb<sub>2</sub>Te<sub>3</sub> superlattices which are shown to be a new type of nanostructured PCMs.

## VI. METHODS

The MBE growth procedure is detailed in our previous publications.<sup>17,18</sup> PVD films were grown from stoichiometric GeTe and Sb<sub>2</sub>Te<sub>3</sub> targets by MaTeck (Juelich, Germany, 3 inch, purity 99.99%). The sputter-guns were powered by 35 W with an Ar flow of 35 sccm yielding a deposition pressure of  $p = 1.6 \times 10^{-2}$  mbar ( $pd = 0.28$  mbar cm with  $d \approx 17.5$  cm the deposition distance). The substrates have been thermalized for 30 min at the deposition temperature (210 °C) prior to deposition. Annealing of films was performed in a tube furnace, where heating and cooling occurred at 5 K/min and held at constant temperature for 30 min under constant Ar flow of 150 sccm.

TEM specimen were prepared by mechanical polishing, dimple-grinding and low-voltage Ar<sup>+</sup> ion-milling with a Gatan PIPS II (Gatan Inc., Pleasanton, California). HAADF-STEM measurements were performed with a JEOL ARM 200F (JEOL Ltd., Tokyo, Japan) with sub-Å settings, where the accelerating voltage was 200 kV, the semi-convergence angle was 22 mrad and ADF collecting angles were 68–280 mrad. The (coherent) TEM measurements were performed with a JEOL 2010F (JEOL Ltd.) and EDX measurements were performed with a JEOL 2010 (JEOL Ltd.) equipped with LN<sub>2</sub>-cooled SiLi detector.

XRD measurements were conducted on a Bruker D8 Discover (Bruker Corporation, Billerica, Massachusetts).  $\theta$ – $2\theta$  scans were performed with a Ge(220) ACC2 monochromator (provided by Bruker Corporation) and

a 0.6 mm detector slit. Pole figure measurements were conducted in skew geometry without detector slits.

Structural models in Fig. 1 are drawn with the VESTA software package.<sup>49</sup>

## ACKNOWLEDGMENTS

This work was supported by EU within the FP7 project PASTRY (GA 317746). Solliance is acknowledged for funding the HRSTEM facility.

## REFERENCES

1. S.R. Ovshinsky: Reversible electrical switching phenomena in disordered structures. *Phys. Rev. Lett.* **21**, 1450 (1968).
2. M. Wuttig and N. Yamada: Phase-change materials for rewriteable data storage. *Nat. Mater.* **6**, 824 (2007).
3. J. Orava, A.L. Greer, B. Gholipour, D.W. Hewak, and C.E. Smith: Characterization of supercooled liquid Ge<sub>2</sub>Sb<sub>2</sub>Te<sub>5</sub> and its crystallization by ultrafast-heating calorimetry. *Nat. Mater.* **11**, 279 (2012).
4. D. Loke, T.H. Lee, W.J. Wang, L.P. Shi, R. Zhao, Y.C. Yeo, T.C. Chong, and S.R. Elliott: Breaking the speed limits of phase-change memory. *Science* **336**, 1566 (2012).
5. S. Raoux, G.W. Burr, M.J. Breitwisch, C.T. Rettner, Y.C. Chen, R.M. Shelby, M. Salinga, D. Krebs, S-H. Chen, H-L. Lung, and C.H. Lam: Phase-change random access memory: A scalable technology. *IBM J. Res. Dev.* **52**, 465 (2008).
6. G.W. Burr, M.J. Breitwisch, M. Franceschini, D. Garetto, K. Gopalakrishnan, B. Jackson, B. Kurdi, C. Lam, L.A. Lastras, A. Padilla, B. Rajendran, S. Raoux, and R.S. Shenoy: Phase change memory technology. *J. Vac. Sci. Technol., B* **28**, 223 (2010).
7. P. Hosseini, C.D. Wright, and H. Bhaskaran: An optoelectronic framework enabled by low-dimensional phase-change films. *Nature* **511**, 206 (2014).
8. C. Ríos, M. Stegmaier, P. Hosseini, D. Wang, T. Scherer, C.D. Wright, H. Bhaskaran, and W.H.P. Pernice: Integrated all-photonic non-volatile multi-level memory. *Nat. Photonics* **9**, 725 (2015).
9. C. Ríos, P. Hosseini, R.A. Taylor, and H. Bhaskaran: Color depth modulation and resolution in phase-change material nanodisplays. *Adv. Mater.* **28**, 4720 (2016). doi: 10.1002/adma.201506238.
10. T. Siegrist, P. Jost, H. Volker, M. Woda, P. Merkelbach, C. Schlockermann, and M. Wuttig: Disorder-induced localization in crystalline phase-change materials. *Nat. Mater.* **10**, 202 (2011).
11. A.L. Lacaita and A. Redaelli: The race of phase change memories to nanoscale storage and applications. *Microelectron. Eng.* **109**, 351 (2013).
12. M. Boniardi, A. Redaelli, C. Cupeta, F. Pellizzer, L. Crespi, G. D'Arrigo, A.L. Lacaita, and G. Servalli: Optimization metrics for phase change memory (PCM) cell architectures. In *Electron Devices Meeting (IEDM), 2014 IEEE International*, 2014; p. 29.1.1. doi: 10.1109/IEDM.2014.7047131.
13. T.C. Chong, L.P. Shi, R. Zhao, P.K. Tan, J.M. Li, H.K. Lee, X.S. Miao, A.Y. Du, and C.H. Tung: Phase change random access memory cell with superlattice-like structure. *Appl. Phys. Lett.* **88**, 122114 (2006).
14. R.E. Simpson, P. Fons, A.V. Kolobov, T. Fukaya, M. Krbal, T. Yagi, and J. Tominaga: Interfacial phase-change memory. *Nat. Nanotechnol.* **6**, 501 (2011).
15. J. Tominaga, P. Fons, A. Kolobov, T. Shima, T.C. Chong, R. Zhao, H.K. Lee, and L. Shi: Role of Ge switch in phase transition: Approach using atomically controlled GeTe/Sb<sub>2</sub>Te<sub>3</sub> superlattice. *Jpn. J. Appl. Phys.* **47**, 5763 (2008).
16. J. Tominaga, T. Shima, P. Fons, R. Simpson, M. Kuwahara, and A. Kolobov: What is the origin of activation energy in phase-change film? *Jpn. J. Appl. Phys.* **48**, 03A053 (2009).
17. J. Momand, R. Wang, J.E. Boschker, M.A. Verheijen, R. Calarco, and B.J. Kooi: Interface formation of two- and three-dimensionally bonded materials in the case of GeTe–Sb<sub>2</sub>Te<sub>3</sub> superlattices. *Nanoscale* **7**, 19136 (2015).
18. B. Casarin, A. Caretta, J. Momand, B.J. Kooi, M.A. Verheijen, V. Bragaglia, R. Calarco, M. Chukalina, X. Yu, J. Robertson, F.R.L. Lange, M. Wuttig, A. Redaelli, E. Varesi, F. Parmigiani, and M. Malvestuto: Revisiting the local structure in Ge–Sb–Te based chalcogenide superlattices. *Sci. Rep.* **6**, 22353 (2016).
19. R. Wang, V. Bragaglia, J.E. Boschker, and R. Calarco: Intermixing during epitaxial growth of van der Waals bonded nominal GeTe/Sb<sub>2</sub>Te<sub>3</sub> superlattices. *Cryst. Growth Des.* **16**, 3596 (2016). doi: 10.1021/acs.cgd.5b01714.
20. B.J. Kooi and J.T.M.D. Hosson: Electron diffraction and high-resolution transmission electron microscopy of the high temperature crystal structures of Ge<sub>x</sub>Sb<sub>2-x</sub>Te<sub>3+x</sub> (x = 1,2,3) phase change material. *J. Appl. Phys.* **92**, 3584 (2002).
21. T. Matsunaga and N. Yamada: Structural investigation of GeSb<sub>2</sub>Te<sub>4</sub>: A high-speed phase-change material. *Phys. Rev. B* **69**, 104111 (2004).
22. T. Matsunaga, N. Yamada, and Y. Kubota: Structures of stable and metastable Ge<sub>2</sub>Sb<sub>2</sub>Te<sub>5</sub>, an intermetallic compound in GeTe–Sb<sub>2</sub>Te<sub>3</sub> pseudobinary systems. *Acta Crystallogr. B* **60**, 685 (2004).
23. T. Matsunaga, R. Kojima, N. Yamada, K. Kifune, Y. Kubota, and M. Takata: Structural investigation of Ge<sub>3</sub>Sb<sub>2</sub>Te<sub>6</sub>, an intermetallic compound in the GeTe–Sb<sub>2</sub>Te<sub>3</sub> homologous series. *Appl. Phys. Lett.* **90**, 161919 (2007).
24. J. Goldak, C.S. Barrett, D. Innes, and W. Youdelis: Structure of alpha GeTe. *J. Chem. Phys.* **44**, 3323 (1966).
25. T.L. Anderson and H.B. Krause: Refinement of the Sb<sub>2</sub>Te<sub>3</sub> and Sb<sub>2</sub>Te<sub>2</sub>Se structures and their relationship to nonstoichiometric Sb<sub>2</sub>Te<sub>3</sub>–ySey compounds. *Acta Crystallogr. B* **30**, 1307 (1974).
26. A.K. Geim and I.V. Grigorieva: Van der Waals heterostructures. *Nature* **499**, 419 (2013).
27. N. Yamada and T. Matsunaga: Structure of laser-crystallized Ge<sub>2</sub>Sb<sub>2+x</sub>Te<sub>5</sub> sputtered thin films for use in optical memory. *J. Appl. Phys.* **88**, 7020 (2000).
28. M. Wuttig, D. Lüsebrink, D. Wamwangi, W. Welnic, M. Gilleßen, and R. Dronskowski: The role of vacancies and local distortions in the design of new phase-change materials. *Nat. Mater.* **6**, 122 (2007).
29. V. Bragaglia, F. Arciprete, W. Zhang, A.M. Mio, E. Zallo, K. Perumal, A. Giussani, S. Cecchi, J.E. Boschker, H. Riechert, S. Privitera, E. Rimini, R. Mazzarello, and R. Calarco: Metal–Insulator transition driven by vacancy ordering in GeSbTe phase change materials. *Sci. Rep.* **6**, 23843 (2016).
30. W. Zhang, A. Thiess, P. Zalden, R. Zeller, P.H. Dederichs, J.-Y. Raty, M. Wuttig, S. Blügel, and R. Mazzarello: Role of vacancies in metal–insulator transitions of crystalline phase-change materials. *Nat. Mater.* **11**, 952 (2012).
31. Y. Jiang, Y.Y. Sun, M. Chen, Y. Wang, Z. Li, C. Song, K. He, L. Wang, X. Chen, Q.-K. Xue, X. Ma, and S.B. Zhang: Fermi-Level tuning of epitaxial Sb<sub>2</sub>Te<sub>3</sub> thin films on graphene by regulating intrinsic defects and substrate transfer doping. *Phys. Rev. Lett.* **108**, 66809 (2012).
32. A.V. Kolobov, P. Fons, A.I. Frenkel, A.L. Ankudinov, J. Tominaga, and T. Uruga: Understanding the phase-change mechanism of rewritable optical media. *Nat. Mater.* **3**, 703 (2004).
33. J. Tominaga, A.V. Kolobov, P. Fons, T. Nakano, and S. Murakami: Ferroelectric order control of the Dirac-semimetal phase in GeTe–Sb<sub>2</sub>Te<sub>3</sub> superlattices. *Adv. Mater. Interfaces* **1**, 1300027 (2014).

34. T. Ohyanagi, M. Kitamura, M. Araidai, S. Kato, N. Takaura, and K. Shiraishi: GeTe sequences in superlattice phase change memories and their electrical characteristics. *Appl. Phys. Lett.* **104**, 252106 (2014).
35. X. Yu and J. Robertson: Modeling of switching mechanism in GeSbTe chalcogenide superlattices. *Sci. Rep.* **5**, 12612 (2015).
36. J.E. Boschker, J. Momand, V. Bragaglia, R. Wang, K. Perumal, A. Giussani, B.J. Kooi, H. Riechert, and R. Calarco: Surface reconstruction-induced coincidence lattice formation between two-dimensionally bonded materials and a three-dimensionally bonded substrate. *Nano Lett.* **14**, 3534 (2014).
37. A.V. Kolobov, J. Tominaga, P. Fons, and T. Uruga: Local structure of crystallized GeTe films. *Appl. Phys. Lett.* **82**, 382 (2003).
38. J. Tominaga, A.V. Kolobov, P.J. Fons, X. Wang, Y. Saito, T. Nakano, M. Hase, S. Murakami, J. Herfort, and Y. Takagaki: Giant multiferroic effects in topological GeTe–Sb<sub>2</sub>Te<sub>3</sub> superlattices. *Sci. Technol. Adv. Mater.* **16**, 14402 (2015).
39. Y. Saito, P. Fons, A.V. Kolobov, and J. Tominaga: Self-organized van der Waals epitaxy of layered chalcogenide structures. *Phys. Status Solidi B* **252**, 2151 (2015). doi: 10.1002/pssb.201552335.
40. A. Koma: Van der Waals epitaxy for highly lattice-mismatched systems. *J. Cryst. Growth* **201–202**, 236 (1999).
41. U. Ross, A. Lotnyk, E. Thelander, and B. Rauschenbach: Microstructure evolution in pulsed laser deposited epitaxial Ge–Sb–Te chalcogenide thin films. *J. Alloys Compd.* **676**, 582 (2016).
42. F. Katmis, R. Calarco, K. Perumal, P. Rodenbach, A. Giussani, M. Hanke, A. Proessdorf, A. Trampert, F. Grosse, R. Shayduk, R. Champion, W. Braun, and H. Riechert: Insight into the growth and control of single-crystal layers of Ge–Sb–Te phase-change material. *Cryst. Growth Des.* **11**, 4606 (2011).
43. K. Perumal: *Epitaxial Growth of Ge–Sb–Te Based Phase Change Materials* (Humboldt-Universität zu Berlin, Mathematisch-Naturwissenschaftliche Fakultät I, Berlin, 2013).
44. R. Venkatasubramanian: Lattice thermal conductivity reduction and phonon localizationlike behavior in superlattice structures. *Phys. Rev. B* **61**, 3091 (2000).
45. J.C. Caylor, K. Coonley, J. Stuart, T. Colpitts, and R. Venkatasubramanian: Enhanced thermoelectric performance in PbTe-based superlattice structures from reduction of lattice thermal conductivity. *Appl. Phys. Lett.* **87**, 23105 (2005).
46. A.V. Kolobov, M. Krbal, P. Fons, J. Tominaga, and T. Uruga: Distortion-triggered loss of long-range order in solids with bonding energy hierarchy. *Nat. Chem.* **3**, 311 (2011).
47. R.E. Simpson, P. Fons, A.V. Kolobov, M. Krbal, and J. Tominaga: Enhanced crystallization of GeTe from an Sb<sub>2</sub>Te<sub>3</sub> template. *Appl. Phys. Lett.* **100**, 21911 (2012).
48. X. Zhou, J. Kalikka, X. Ji, L. Wu, Z. Song, and R.E. Simpson: Phase-change memory materials by design: A strain engineering approach. *Adv. Mater.* **28**, 3007 (2016).
49. K. Momma and F. Izumi: VESTA 3 for three-dimensional visualization of crystal, volumetric and morphology data. *J. Appl. Crystallogr.* **44**, 1272 (2011).